Characterization of Transport Across Cellulose Acetate Membranes in the Presence of Strong Solute–Membrane Interactions

H.-G. BURGHOFF, K. L. LEE,* and W. PUSCH, *Max-Planck-Institut für Biophysik, 6000 Frankfurt am Main 70, Germany*

Synopsis

Certain organic solutes, including phenol, undergo anomalous enrichment when hyperfiltered through cellulose acetate membranes: the solute concentration is higher in the permeate than in the feed solution. A number of existing theoretical approaches describing hyperfiltration phenomena are presented and their merits and limitations upon application to the transport of phenol discussed. A new two-parameter transport relationship is derived based on an extension of the solution–diffusion model. The enrichment, or negative solute rejection by the membrane, is predicted to occur whenever the pressure-induced solute permeation velocity exceeds that of water. By acknowledging and incorporating the effect of pressure on the chemical potential of the solute, the present extended solution–diffusion model relationship successfully describes hyperfiltration data of phenol in homogeneous and asymmetric cellulose acetate membranes provided the contribution of convective flow to the overall solute transport is insignificant. In addition to the transport parameters of the extended solution–diffusion model, the transport parameters of the phenomenological, Kedem–Spiegler, and combined viscous flow–frictional relationship are evaluated from hyperfiltration data obtained with 0.05 and 0.1 wt % phenol feed solutions and homogeneous cellulose acetate membranes of different acetyl content.

INTRODUCTION

Cellulose acetate (CA) membranes have assumed a dominant role in desalination applications since the infancy of hyperfiltration (reverse osmosis) technology. The characteristic large difference between permeabilities of CA membranes to water and inorganic salts was exploited to advantage by fabricating the polymer into asymmetric membranes which, with their submicron effective barrier thickness, provide water fluxes high enough to realize commercial desalination by the pressure-driven process. In fact, the past two decades have seen intense research activities focused on the transport behavior of various inorganic salts in asymmetric CA membranes. The generally successful separation of salts (measured by the normalized concentration difference between feed and permeate solutions and conventionally termed "solute rejection") has, in turn, widened the scope of study to include simple organic compounds such as ketones, alcohols, etc.[1,2] In most cases CA membranes provide some degree of rejection of organic substances, depending upon their chemical classification.

Phenol is one of a few notable exceptions. Under conventional hyperfiltration conditions, phenol concentrations in the permeate have been repeatedly found to exceed those in the feed solution.[3–8] The term "negative rejection" is coined for this enrichment phenomenon. The cause of negative rejection has been attributed to significant solute–membrane interactions.[3,6,8,37] Neither the classical

* Present address: Bend Research, 64550 Research Road, Bend, Oregon 97701.

Journal of Applied Polymer Science, Vol. 25, 323–347 (1980)

0021-8995/80/0025-0323$01.00

solution–diffusion model[36] nor the common finely porous membrane model[10] offers a consistent quantitative explanation of negative rejection in terms of solute partition and diffusion coefficients. Recently, Jonsson[7] applied a combined viscous flow–frictional model to characterize the hyperfiltration of organic compounds. The transport parameters derived could be used to predict the behavior of the membranes with reasonable success.

Another possible approach involves membrane-model-independent transport relationships based on the thermodynamics of irreversible processes. Although widely applied to analyzing hyperfiltration data of inorganic salts,[11–15] these relationships have only recently been employed to study the transport of organic compounds.[7,8]

An alternative, two-parameter relationship based on an extension of the classical solution–diffusion model, is presented in this paper. By considering the pressure-dependent part of the chemical potential of the solute, $\overline{V}_s \Delta P$, diffusive transport is correlated to concentration and pressure gradients. It will be demonstrated that this model is applicable to hyperfiltration data of phenol in homogeneous and asymmetric CA membranes when the contribution of convective flow to the overall solute transport is negligibly small.

THEORY

Certain membrane transport relationships are completely general, independent of membrane models and assumptions. Others are based upon specific membrane models; thus, their applicability depends on the condition that certain model assumptions be satisfied.

Examples of model-independent treatments are the phenomenological and Kedem–Spiegler nonlinear relationships,[16,17] whereas model-dependent ones include those based on the finely porous membrane model,[9,10] the combined viscous flow–frictional model,[18] and the new extended solution–diffusion model presented in this paper. In each case the necessary transport parameters can be computed from the pressure and concentration dependencies of rejection and volumetric flux.

Phenomenological Transport Relationship

It was recently shown that the reciprocals of the solute rejection r and volume flux q are linearly related by the following equation[16]:

$$\frac{1}{r} = \frac{1}{r_\infty} + \frac{(l_\pi/l_p - r_\infty^2) l_p \Pi'}{r_\infty} \frac{1}{q} \tag{1}$$

where $r = (c_s' - c_s'')/c_s'$ = solute rejection; c_s' = feed solute concentration (mole/l. or mole/cm^3); c_s'' = product (filtrate) solute concentration (mole/l. or mole/cm^3); r_∞ = asymptotic solute rejection at infinitely large volume flux, corresponding to an infinite transmembrane pressure drop ΔP; l_p = hydrodynamic permeability of the membrane (cm/sec atm); l_π = osmotic permeability of the membrane (cm/sec atm); Π' = osmotic pressure of the feed solution (atm); and q = volume flux across the membrane (g/cm^2 sec or cm/sec).

Equation (1) is derived from irreversible thermodynamics, where the only necessary assumption involves defining some mean solute concentration $\tilde{c}_s$ in

the expression of the corresponding solute flux in the absence of exact concentration profile information. The definition of $\tilde{c}_s$ is related to the problem of splitting the solute flux Φ_s across the membrane of a discontinuous description into convective and diffusive components.[16,19]

A second relationship exists between volume flux and the effective pressure difference, $\Delta P - \sigma\Delta\Pi$:

$$q = l_p(\Delta P - \sigma\Delta\Pi) \tag{2}$$

where σ = reflection coefficient of the membrane, equal to r_∞ under the assumption that $\tilde{c}_s = c_s'$; $\Delta P = P' - P''$ = hydrostatic pressure difference across the membrane (atm); and $\Delta\Pi = \Pi' - \Pi''$ = osmotic pressure difference across the membrane (atm).

Employing the relationship $\sigma = r_\infty$, inherent in the Kedem–Spiegler and the phenomenological relationships, and the approximation $\Delta\Pi \simeq r\Pi'$, eq. (2) may be rewritten in the more convenient form

$$q = l_p(\Delta P - r_\infty \Delta\Pi) \simeq l_p(\Delta P - r_\infty r\Pi') \tag{2a}$$

Measuring r and q as functions of the pressure difference ΔP at a constant solute concentration c_s', the transport parameters l_p, l_π, and r_∞ can be obtained from the $1/r$ vs. $1/q$ and q vs. ΔP plots by linear regression analysis.

Nonlinear Relationship of Kedem and Spiegler

Kedem and Spiegler[17] suggested that the conditions of large concentration and pressure differences across a membrane in hyperfiltration experiments may cause the linear range of the relationships of thermodynamics of irreversible processes to be exceeded. These authors therefore derived a set of differential equations from the original linear ones. Integrating these differential equations with the customary boundary conditions of hyperfiltration yields the following relationships for the solute rejection and the volume flux:

$$\frac{1}{1-r} = \frac{1}{1-r_\infty} - \frac{r_\infty}{1-r_\infty} \exp\left\{\frac{-q(1-r_\infty)d}{P_s}\right\} \tag{3}$$

$$q = \frac{P_w}{d}(\Delta P - r_\infty \Delta\Pi) \tag{4}$$

where d = membrane thickness (cm); P_w = water permeability of the membrane (cm^2/sec atm); and P_s = solute permeability of the membrane (cm^2/sec). The transport parameters P_w, P_s, and $r_\infty = \sigma$ are obtained by least-squares analysis of the corresponding r and q data as functions of ΔP at a constant solute concentration c_s' of the feed solution.

Finely Porous Membrane Model Relationship

The finely porous membrane model was introduced by Schmid[9] and used by Schlögl[10] for treating theoretically the transport of solutes and solvents across ion exchange membranes by means of the Nernst–Planck equations. In case of a binary nonelectrolyte solution, the following relationships are obtained:

$$\frac{1}{1-r} = \frac{1}{K_s'} - \frac{1-K_s''}{K_s'} \exp\left(\frac{-q\delta}{D_{sm}}\right) \tag{5}$$

$$q = \frac{d_h}{\delta}(\Delta P - \sigma\Delta\Pi) \tag{6}$$

where d_h = hydrodynamic permeability coefficient (cm^2/sec atm); $\delta = td$ = path length of the pores in the membrane (cm); t = tortuosity factor; and D_{sm} = diffusion coefficient of solute within the membrane (cm^2/sec). As $q \rightarrow \infty$, eq. (5) yields

$$r_\infty = 1 - K_s' \tag{7}$$

The asymptotic rejection r_∞ is thus only determined by the partition coefficient of the solute, K_s'.

The Kedem–Spiegler and finely porous membrane model relationships have the same analytical form. Therefore, the transport parameters of these relationships can be correlated to each other.[11,16] For example, assuming $K_s' = K_s''$, the following relations result:

$$r_\infty = \sigma = 1 - K_s' \tag{7a}$$

$$\frac{P_s}{d} = \frac{K_s' D_{sm}}{\delta} \tag{7b}$$

Combined Viscous Flow and Frictional Model Relationship

Using a balance of applied and frictional forces as proposed by Spiegler,[20] Merten[18] arrived at the following relationships:

$$\frac{1}{1-r} = \frac{b}{K_s'} - \frac{b - K_s''}{K_s'} \exp\left(\frac{-q\delta f_{sw}}{RT}\right) \tag{8}$$

$$q = \frac{d_h^0}{\delta\eta}(\Delta P - \sigma\Delta\Pi) \tag{9}$$

where $b = 1 + (f_{sm}/f_{sw})$ = drag factor; f_{sw} = friction coefficient characterizing the friction between a mole of solute and an infinite amount of water (g/sec mole); f_{sm} = friction coefficient characterizing the friction between solute and the membrane matrix (g/sec mole); η_0 = viscosity of pure solvent (water) (g/cm sec); $\eta = \eta_0\{1 + (d_h^0 f_{sm}/M_s)c_s''\}$ = viscosity of solution (g/cm sec); d_h^0 = hydrodynamic permeability coefficient of pure solvent (cm^2/sec atm); M_s = molecular weight of solute (g/mole); R = gas constant (l. atm/mole degree); and T = absolute temperature (K).

For volume fluxes approaching infinity, corresponding to very high pressure differences, the exponential term in eq. (8) vanishes. Thus,

$$r_\infty = 1 - \frac{K_s'}{b} \tag{10}$$

The viscous flow–frictional model therefore predicts that the asymptotic solute rejection is determined by both the solute partition coefficient K_s' and the drag factor b. In case there is no solute–membrane frictional interaction, $f_{sm} = 0$, so that $b = 1$ and the asymptotic solute rejection coincides with that predicted by the simple finely porous membrane model relationship. On the other hand, if there is no interaction between the solute and solvent, $f_{sw} = 0$, so that $b \rightarrow \infty$ and the solution–diffusion case results where $r_\infty = 1$.

Extended Solution–Diffusion Model Relationship

The regular solution–diffusion model as developed by Merten et al.[18] requires that $r_\infty = 1$ under all circumstances. Therefore, this transport model cannot explain negative solute rejection, $r_\infty < 0$. In his derivation Merten assumed that the product of the partial molar volume of solute and the applied pressure difference $\overline{V}_s \Delta P$ in the expression of the chemical potential of the solute can be neglected compared to the term $RT \ln (c_s'/c_s'')$. As has been shown by Clark,[21] the term $\overline{V}_s \Delta P$ may indeed be neglected in hyperfiltration as long as $|\ln (c_s'/c_s'')| \gg 8 \times 10^{-4}\ \Delta P$ (atm), which is true for salt solutions. However, in cases of phenol and other organic solutes, this inequality is modified to $|\ln (c_s'/c_s'')| \gg 4 \times 10^{-3}\ \Delta P$ because of the larger partial molar volume of phenol. This condition is no longer fulfilled in case of phenol–water solutions since $c_s' \simeq c_s''$. It will be demonstrated that an improved transport relationship can be obtained which allows for negative solute rejection by taking into account the pressure term of the chemical potential of the solute.

According to the assumption underlying the solution–diffusion model, no coupling exists between solute and solvent fluxes. That is, the solute and solvent fluxes are independent of each other and are related only to their respective chemical potential differences across the membrane, $\Delta\mu_s$ and $\Delta\mu_w$. The corresponding phenomenological relationships, relating generalized fluxes to conjugated generalized forces, are as follows:

$$\Phi_w = \frac{L_w}{d} \Delta\mu_w = \left(\frac{L_w \overline{V}_w}{d}\right)(\Delta P - \Delta\Pi) \tag{11}$$

$$\Phi_s = \frac{L_s}{d} \Delta\mu_s = \frac{L_s}{d}\left(\frac{\Delta\Pi}{\tilde{c}_s} + \overline{V}_s\, \Delta P\right) \tag{12}$$

where Φ_w = water flux across the membrane (mole/cm^2 sec or g/cm^2 sec); Φ_s = solute flux across the membrane (mole/cm^2 sec); $\overline{V}_w$, $\overline{V}_s$ = partial molar volume of water and solute, respectively (cm^3/mole); L_w, L_s = phenomenological coefficients (mole^2/cm^4 sec atm); $\tilde{c}_s = \Delta\Pi/\Delta_c\mu_s$ = mean solute concentration (mole/l. or mole/cm^3); $\Delta_c\mu_s \simeq RT \ln (c_s'/c_s'')$ = concentration-dependent part of the chemical potential difference of the solute across the membrane for dilute solutions (activity = concentration; J/mole); $\Delta\mu_w$, $\Delta\mu_s$ = chemical potential difference of water and solute, respectively, across the membrane (J/mole or cm^2 atm/mole); and $\Delta\mu_w = \overline{V}_w(\Delta P - \Delta\Pi)$.

Let $q \simeq \overline{V}_w \Phi_w$ and $(L_s RT/\tilde{c}_s) = P_s = K_s D_{sm}$. Then, by introducing a new transport parameter, $l_{sp} = \overline{V}_s L_s/d$, relationships (11) and (12) can be rewritten as follows:

$$q = l_p(\Delta P - \Delta\Pi) \tag{11a}$$

$$\Phi_s = \frac{K_s D_{sm}}{d} \Delta c_s + l_{sp}\, \Delta P \tag{12a}$$

where l_p is again the hydrodynamic permeability of the membrane, equal to $L_w \overline{V}_w^2 d$. Employing the boundary condition $c_s'' \simeq \Phi_s/q$ at the low-pressure side of the membrane, the solute rejection can be written as $r = 1 - (\Phi_s/c_s' q)$. After some algebraic rearrangement, the following relationship results:

$$\frac{1}{r}\left\{1 - \frac{l_{sp}}{c_s' l_p}\left(1 - \frac{\Delta\Pi}{\Delta P}\right)\right\} = 1 + \frac{P_s}{d}\frac{1}{q} \tag{13}$$

If $(\Delta\Pi/\Delta P) \ll 1$, eq. (13) can be simplified to give

$$\frac{1}{r} = \frac{1}{r_\infty} + \frac{P_s}{d}\frac{1}{r_\infty q} \tag{14}$$

where

$$r_\infty = 1 - \frac{l_{sp}}{c_s' l_p} \tag{15}$$

is again the asymptotic solute rejection. As is obvious from relation (15), a negative solute rejection will result whenever $(l_{sp}/c_s' l_p) > 1$, that is, whenever the pressure-induced solute permeation velocity $l_{sp}\Delta P/c_s'$ is higher than the pressure-induced water permeation velocity $l_p \Delta P$. The two transport parameters l_p and P_s/d may therefore be used as the independent variables in a relationship which can be applied to hyperfiltration systems exhibiting negative solute rejection.

The transport parameter l_{sp} may be written

$$l_{sp} = \frac{D_{sp}}{RTd(\bar{V}_w/\bar{V}_s)} \tag{16}$$

where D_{sp} is a "pressure diffusion coefficient" of the solute, as defined by Haase[22] and Schlögl,[25] comparable to the solute permeability P_s, and is related to the original transport parameter L_s by $D_{sp} = L_s RT\bar{V}_w$. Therefore, D_{sp} is not an independent third transport parameter but can rather be correlated to the solute diffusion coefficient within the membrane, D_{sm}, by

$$\frac{D_{sp}}{D_{sm}} = K_s \tilde{c}_s \bar{V}_w \tag{17}$$

Using the definitions of l_{sp} and P_s/d, this relationship can be transformed into the following equivalent one:

$$\frac{l_{sp}}{P_s/d} = \frac{\tilde{c}_s \bar{V}_s}{RT} \tag{17a}$$

In the same way, a diffusion coefficient for water within the membrane is defined[25] by

$$D_w = \frac{l_p RTd}{\bar{V}_w} \tag{18}$$

This water diffusion coefficient is related to the membrane-fixed reference system. As Prigogine pointed out,[23] this diffusion coefficient does not characterize the thermal motion of water molecules alone but may also include pressure- and/or osmotic pressure-driven convective motion of water. In order to arrive at a purely thermal diffusion coefficient characterizing only the Brownian motion of the water molecules, the local center of mass-fixed reference system must be considered. The following relationship holds between the water diffusion coefficient D_w and the one[24] related to the barycentric motion, D_w^*:

$$D_w^* = D_w(1 - w)^2 \tag{19}$$

where w is the water content of the membrane (g H_2O/g wet membrane).

Alternatively, the diffusion coefficient D_w can be correlated with the pore radii in the case of pore flow, as Schlögl[25] showed, by the equation

$$D_w = \frac{a^2 RT}{8\eta \overline{V}_w} \tag{20}$$

where a is the mean pore radii (cm) of the cylindrical pores of the membrane. At very low water contents w of the membrane, eq. (19) yields $D_w^* \simeq D_w$. On the other hand, at high water contents, $w \to 1$ corresponding to $a \to \infty$, and D_w will itself approach infinity ($D_w \to \infty$ at $w \to 1$). Therefore, the product $D_w(1 - w)^2$ is likely to approach a limiting value at $w \to 1$, and this should be the self-diffusion coefficient of water in free solution.

In order to illustrate the effect of the partial molar volume of a solute on the pressure diffusion coefficient, a two-component system might be considered. The solute diffusion coefficient D_s and the solute pressure diffusion coefficient D_p of such a two-component system are related to $(\partial\mu/\partial x_s)_{T,P}$, the partial differential of the chemical potential with respect to the mole fraction of the solute, x_s, at constant temperature and pressure. Assuming the mole fraction of water to be approximately 1 ($x_w \simeq 1$), the following expression results (ref. 22, eq. 12c):

$$\frac{D_p}{D_s} \simeq \frac{M_w M_s RT}{(M_w + x_s M_s)} \left(\frac{\overline{V}_s}{\overline{V}_w} - 1 \right) \frac{1}{(\partial\mu_s/\partial x_s)_{T,P}} \tag{21}$$

where x_s is the mole fraction of the solute and M_w and M_s are the molecular weights of water and the solute, respectively. In a two-component system, the sign of D_P is thus determined by that of $\overline{V}_s - \overline{V}_w$ since D_s is always positive. The component with the higher partial molar volume will move to a location of lower pressure, as is obvious from eq. (12).

EXPERIMENTAL

In order to verify the validity of special membrane model relationships, it is necessary to determine the transport and equilibrium parameters inherent in the model by independent measurements. For that reason, the diffusion and partition coefficients of phenol were determined for homogeneous CA membranes. In addition, the hyperfiltration performance of asymmetric and homogeneous CA membranes cast from CA of different acetyl content has been investigated. From the results of these experiments, the transport coefficients of several transport relationships were evaluated.

Homogeneous Cellulose Acetate Membranes

The homogeneous CA membranes were cast from chloroform solutions of Bayer Cellits F-700, K-700, and L-700 and Eastman–Kodak CA E-320 with 40.1, 39.1, 38.4, and 32.0% acetyl content, respectively. The membranes were cast at 30°C and then dried at the same temperature in an air-conditioning system (Vötsch Company, Frommern, Germany). The thickness of the final membranes ranged from 5 to 10 μm. Only one membrane, prepared from Cellit K-700, had a final thickness of about 25 μm.

Asymmetric Cellulose Acetate Membranes

The asymmetric CA membranes were cast according to the procedure of Manjikian, Loeb, and McCutchan[26] using solutions of Bayer Cellit K-700 in acetone–formamide mixtures. The membranes were cast on glass plates in an air-conditioning system at 25°C and 65% relative humidity. After an evaporation period of about 30 sec, the membranes were immersed in water of 25°C for about 1 hr. The water was repeatedly renewed. The final thickness of the wet membranes was about 100 μm. The membranes were than annealed in a water bath at 60, 75, 80, 82.5, 85, and 90°C and respectively designated CA-60, CA-75, CA-80, CA-82.5, CA-85, and CA-90.

Phenol and Water Sorption

The sorption of phenol and water by homogeneous and unannealed asymmetric CA membranes as functions of the phenol concentration in the external solution was measured at 25 and 45°C applying the following experimental procedure. Appropriate CA membrane samples were soaked in aqueous phenol solutions ranging in phenol concentrations from 0.1 to 100 mmole/l. Thermodynamic equilibrium was assumed to be established after seven days.[8] Two membrane samples of about 150 mg each were removed from the solution, blotted with tissue paper, and then weighed using an analytical balance accurate to ±0.1 mg (Sartorius, Göttingen, Germany). One sample was used to determine the wet and dry weights of the membrane and thus the water regain. The second sample was analyzed for its phenol content by dissolving the membrane in trimethyl phosphate and then measuring the UV absorbance of that solution at 270 nm against a reference solution of a phenol-free membrane sample in the same solvent. The dry weights of the sample membranes were obtained by drying the samples at 120°C until constant weights were achieved (one to two days). A chemical analysis of the dried sample membranes showed a removal of 99% of the sorbed water and phenol.[8]

Using the wet and dry weights as well as the measured phenol content of the sample membrane, the water content v (mg H_2O/100 mg dry membrane) and the phenol content u (mg phenol/100 mg dry membrane) of each membrane were obtained. The partition coefficient of phenol, K_s, was then calculated from the phenol and water contents of the sample membrane as follows:

$$K_s = \frac{10u}{M_s c_s\,(1 + 0.01v)} = \frac{10u_w}{M_s c_s} \tag{22}$$

where M_s = 94.11 g/mole is the molecular weight of phenol and u_w is the phenol content in wt % phenol referred to the wet weight of the sample membrane (mg phenol/100 mg wet membrane). The partition coefficient K_s was obtained in units of (mole/kg wet membrane)/(mole/kg solution) if the units of u, u_w, and v are wt % and those of c_s are mole/kg solution. In order to quantify the sorption of phenol by an analytical relationship, a sorption model can be used as discussed in Appendix B.

Solute Diffusion Coefficient and Permeability from Dialysis Experiments

The permeability P_s and the diffusion coefficient D_{sm} of phenol in a homogeneous CA membrane were measured using a dialysis cell, described in detail elsewhere.[27] The homogeneous CA membrane sample of effective membrane area $A = 0.636$ cm^2 was placed into the membrane holder of the dialysis cell separating a phenol solution, (′)-phase, from pure water, (″)-phase, at the beginning of each experimental run. The solutions in both cell compartments were well stirred and maintained under constant atmospheric pressure ($P' = P''$). The dialysis cell was placed into a thermostatted water bath at 25°C. The CA membrane samples used were always equilibrated in phenol–water solutions of phenol concentration c_s' for about ten days before being mounted into the membrane holder of the dialysis cell. The permeation experiments were repeated using different phenol concentrations c_s' (1 mmole/l. up to 100 mmole/l.). No volume flow across the membrane was observed. The variation of the phenol concentration c_s'' of the (″)-phase with time was followed by analyzing the (″)-phase at 1-hr intervals. The sample solutions taken from the (″)-phase were always returned to the same compartment after each concentration determination in order to maintain a constant volume of $V'' = 50$ ml. The phenol concentration c_s'' varied linearly with the time t, whereas the concentration c_s' remained nearly constant during an experimental run. Plotting then c_s'' as a function of t resulted in a straight line the slope of which yielded the corresponding constant phenol flux $\Phi_s = (V''/A)(dc_s''/dt)$. Applying Fick's law,

$$\Phi_s = P_s \frac{\Delta c_s}{d} \tag{23}$$

and taking into account $c_s'' \ll c_s'$ and $V'' \simeq$ constant, the following relationship is obtained:

$$\frac{dc_s''}{dt} = \frac{P_s A}{V'' d} c_s' \tag{24}$$

Using the independently measured partition coefficient K_s of phenol, the diffusion coefficient D_{sm} of phenol in the membrane is obtained from $P_s = K_s D_{sm}$. The diffusion coefficient thus calculated refers to the geometric membrane area A. Dividing D_{sm} by the water content w' or the porosity ϵ of the membrane yields D_{sm}', the diffusion coefficient of phenol within the water phase of the membrane.

Hyperfiltration Experiments

Hyperfiltration experiments were carried out using equipment described previously in detail.[14] In order to avoid sorption of phenol by plastic parts, the equipment was modified to contain only stainless steel components. Six hyperfiltration cells were used, each having an effective membrane area of $A \simeq 12$ cm^2. The high-pressure compartments of the six cells were connected in series to the feed stream to give a flow velocity of up to 4 m/sec, thus minimizing concentration polarization effects. Each product stream was individually sampled and analyzed. A thermostatted water bath maintained the system temperature

constant at 25 ± 0.1°C. The feed pressure employed ranged from $P' = 10$ atm up to $P' = 100$ atm.

Each series of hyperfiltration experiments was started employing virgin CA membranes prepressurized using pure water as the feed at 100 atm for three days in order to minimize subsequent compaction effects.[28] Tests were conducted with phenol feed solutions at a concentration of $c_s' = 0.05$ or 0.10 wt % phenol. Steady-state transport was achieved after at least one week. Therefore, a ten-day period was allowed before flux and rejection were measured. The feed solution within the hyperfiltration system was replaced each day during this period to maintain a constant feed phenol concentration. The steady-state volume flux q and the solute rejection r were determined as functions of the applied pressure P'. The phenol concentrations of the feed and product solutions were determined by means of a differential refractometer (manufactured by Waters Associates GmbH, Königstein/Ts., Germany) and for verification by UV spectrometry at 270 nm using a Zeiss DMR-10 spectrophotometer (Carl Zeiss, Oberkochem, Germany).

RESULTS AND ANALYSIS

Sorption of Phenol and Water

The experimentally established phenol and water contents of a homogeneous CA membrane are presented as functions of the external phenol concentration in Figures 1 and 2 for 25 and 45°C, respectively. As reported previously,[8] a homogeneous and an asymmetric CA membrane sorb the same amount of phenol when the comparison is made on a dry weight basis, suggesting that phenol is sorbed by interaction with the polymer chains independent of the membrane structure. Supporting this concept, the sorption model parameters u_m and $1/a$ have been calculated plotting log u vs. log c_s and performing a regression line analysis as discussed in detail in Appendix B. The results are summarized in Table I. The values of the interaction parameter e, characterizing the gain in molar surface energy, were calculated using eq. (24).

The phenol and water contents for homogeneous CA membranes with different acetyl contents were determined at a phenol concentration in the external solution of 0.05 wt %. The corresponding data are compiled in Table II. With decreasing acetyl content of the membrane, the water content v increases while the phenol uptake u decreases, resulting in a net decrease in the partition coefficient of phenol. The further discussion in this section will only be related to the sorption behavior of the CA membranes prepared from cellulose acetate Bayer Cellit K-700.

As can be seen from Figure 1, excellent agreement is achieved between experimental sorption data and the calculated isotherms using the derived parameters u_m and $1/a$. The gain in molar surface energy from sorption is temperature independent within the temperature interval studied. However, the value of the parameter u_m, characterizing the amount of phenol which would be sorbed at an external phenol concentration of $c_s = 1$ mole/l., is projected to increase slightly with increasing temperature. The value of $e = 735$ cal/mole is somewhat larger compared to the gain in molar surface energy by the sorption of water of $e = 666$ cal/mole.[29] This higher energy level probably arises from

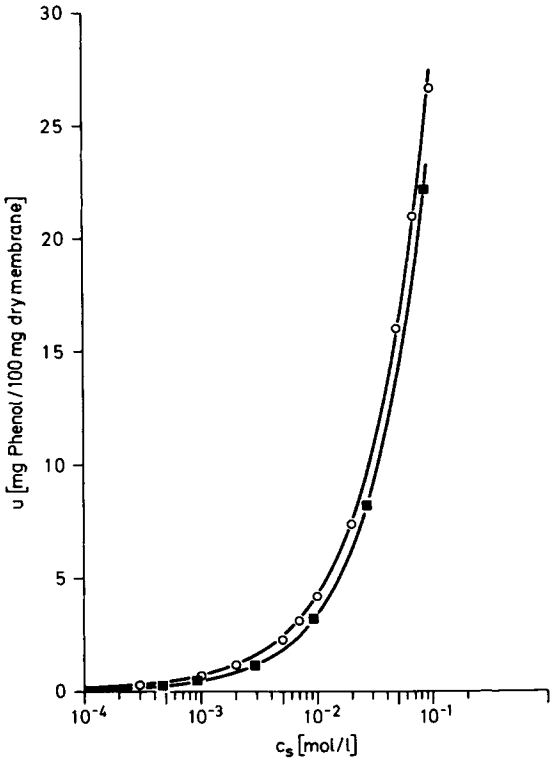

Fig. 1. Phenol content u of a homogeneous cellulose acetate membrane as function of the phenol concentration in the external solution c_s at 25°C (○) and 45°C (■). The curves drawn have been calculated employing eq. (B-1) and the corresponding parameters a and u_m.

a stronger interaction of phenol with the polar groups of the CA chains and the accompanying displacement of some of the water molecules originally bound to those polar groups.[30] It is possible that the attachment of phenol molecules alters the nature of these sorption sites so that additional sorption of water or phenol to form multilayers becomes unfavorable because of steric hindrance and

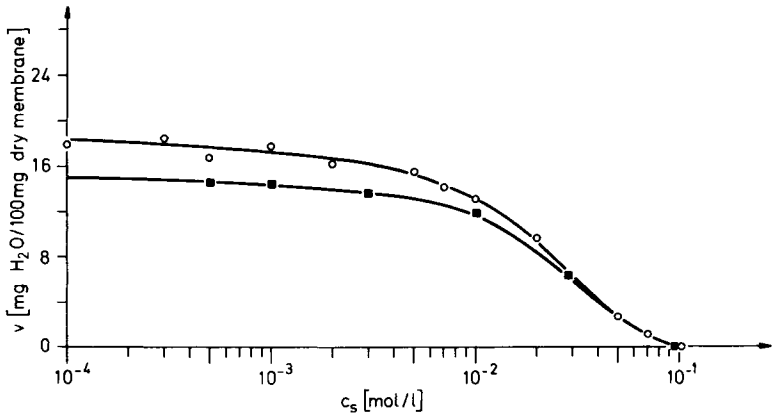

Fig. 2. Water content v of a homogeneous cellulose acetate membrane as function of the phenol concentrations in the external phenol solution c_s at 25°C (○) and 45° (■).

TABLE I
Values of the Model Parameters $1/a$, u_m, and e Characterizing Phenol Sorption in Asymmetric and Homogeneous Cellulose Acetate Membranes (K 700) at 25°C and 45°C

T (K)	u_m (wt-%)	$1/a$	e (cal/mole)
298	174.2	0.810	735.8
318	179.5	0.865	735.3

the nonpolar nature of the phenyl ring. Therefore, as sorption of phenol progresses, the water content of the CA membrane decreases. The water content v of a homogeneous CA membrane is practically independent of the external phenol concentration at $c_s < 10^{-3}$ mole/l. but decreases with increasing external phenol concentration beyond 10^{-3} mole/l. In fact, at an external phenol concentration of about 0.1 mole/l., sufficient phenol is sorbed into the CA polymer to displace all the water in the membrane, yielding an effective water content of nearly zero, as shown in Figure 2.

Figure 3 is a cross-plot of Figures 1 and 2, correlating the water content v to the phenol content u of a homogeneous CA membrane at two different temperatures. Clearly, the water content is inversely related to the phenol content at phenol contents below about 10 wt % for 25°C and below about 8 wt % for 45°C. Both these phenol contents correspond to an external phenol concentration of $c_s = 3 \times 10^{-2}$ mole/l. phenol. At higher external phenol concentrations, the water content of the membrane becomes much lower. It should be mentioned in this connection that CA membranes dissolve in aqueous phenol solutions beyond about 0.1 mole/l. The linear change of v with u at smaller external phenol concentrations agrees with the concept of phenol sorption outlined above. Using the slopes of the linear portion of the v vs. u curves (Fig. 3) and the molecular weights of water, M_w = 18.01 g/mole, and phenol, M_{ph} = 94.11 g/mole, the number of water molecules replaced by one phenol molecule can be calculated

TABLE II
Partition Coefficient K_s, Water Content v, and Phenol Content u_w for Homogeneous Cellulose Acetate Membranes of Varying Acetyl Content at an External Phenol Concentration of c_s = 0.05 wt % at 25°C

Membrane	T 900	F 700	K 700	L 700	E 320
Acetyl content (wt-%)	43.7	40.1	39.1	38.4	32.1
$K_s \left(\frac{\text{mol / kg wet membrane}}{\text{mol / kg solution}}\right)$	60.8	51.0	40.0	34.1	19.0
u_w (wt-%) [a]	3.04	2.55	2.00	1.71	0.95
v (wt-%) [b]	7.60	11.9	13.4	14.1	24.05
w' (g H_2O / cm^3 wet membrane)	0.088	0.134	0.150	0.157	0.241
w (g H_2O / g wet membrane)	0.068	0.105	0.118	0.124	0.194

[a] referred to wet membrane weight [b] referred to dry membrane weight

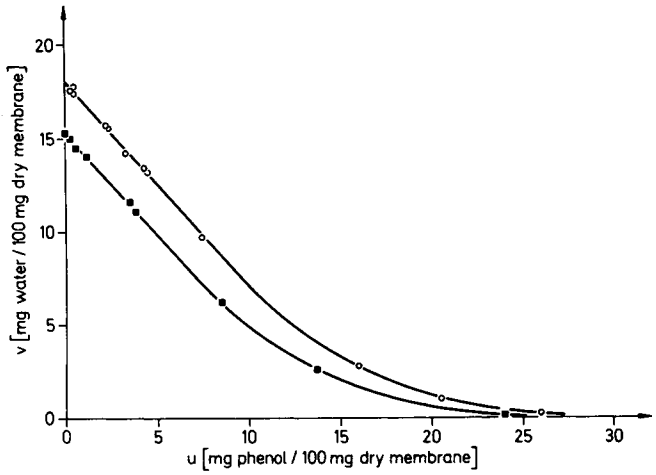

Fig. 3. Cross-plot of Figs. 1 and 2, correlating the water content v to the phenol content u of a homogeneous cellulose acetate membrane at 25°C (○) and 45°C (■).

to be about five at both temperatures. Thus, one phenol molecule is assumed to occupy the volume of five water molecules, in agreement with the relative partial molar volumes of these two substances. The attachment of a phenol molecule at a sorption site shields the attractive forces of that site, rendering attachment of a second layer more difficult because of steric hindrance. By the same reasoning, the volume available for the sorption of solute or solvent molecules within the CA membranes is diminished if larger molecules are sorbed in the first layer. Both of these effects result in a poor sorption ability of the system after the first layer is occupied by large sorbed molecules.

At external phenol concentrations beyond 0.03 mole/l. a nonlinear relationship results between water content and phenol content. The onset of this nonlinearity coincides with the strong decay of the water content of the membrane and also a stronger swelling of the membrane. Further phenol uptake by the membrane leads then to a dissolution of the membrane at external phenol concentrations beyond 0.1 mole/l. At these external phenol concentrations the surface area of the CA membrane no longer remains constant, and therefore the sorption of phenol and water cannot be described by the sorption model presented in Appendix B at concentrations beyond 0.1 mole/l. phenol.

The water content of an unannealed asymmetric CA membrane is found to decrease from about 200 mg/100 mg dry membrane to about 180 mg/100 mg dry membrane within the range of external phenol concentrations used. The large difference between the water content of an asymmetric and a homogeneous CA membrane was shown to be due to capillary water contained in the larger pores of the sublayer matrix in an asymmetric CA membrane.[31,32] Assuming that only the water sorbed by interaction with the polymer chains (sorption sites) of an asymmetric CA membrane is partially or completely replaced by phenol, the comparably small variation of the water content of an asymmetric CA membrane with increasing phenol concentration in the external solution would be due to a nearly constant amount of the capillary water within the porous matrix of the asymmetric CA membrane. The water sorbed by interaction is about 15 wt %, whereas the capillary water makes up about 53 wt % of the overall water content of an asymmetric CA membrane at 100% regain.

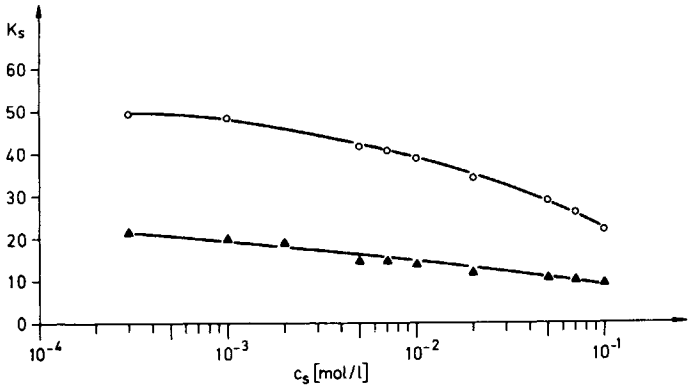

Fig. 4. Partition coefficient K_s of phenol for a homogeneous (O) and an unannealed asymmetric (▼) cellulose acetate membrane as function of the external phenol concentration c_s at 25°C.

Using the results of the sorption measurements, the partition coefficients of phenol for a homogeneous and an unannealed asymmetric CA membrane at 25°C are obtained as functions of the external phenol concentration. The results are shown in Figure 4. A clear difference exists between the partition coefficients of phenol in homogeneous and asymmetric CA membranes. As the distribution coefficient is computed based on the wet weight of the membrane, this difference is a consequence of the excess water within the porous sublayer of asymmetric CA membranes.

Solute Diffusion Coefficient

Experimentally determined values of phenol permeabilities P_s are shown in Figure 5 as a function of the external phenol concentration c_s. Also shown are the diffusion coefficients of phenol within the membrane, calculated from P_s and K_s by means of eq. (26). Since D_{sm} remains constant, independent of c_s, the decrease in P_s with increasing c_s is a consequence of the lower value of K_s at the higher concentrations. The mean value of the phenol diffusion coefficient within a homogeneous CA membrane is $D_{sm} = (1.4 \pm 0.1) \times 10^{-9}$ cm^2/sec, in very good agreement with the results previously obtained by Merten et al.[3] If the

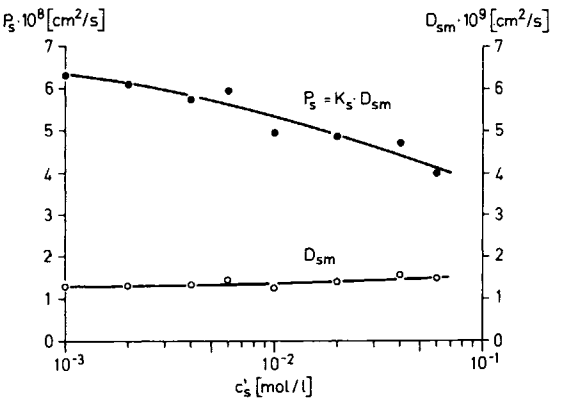

Fig. 5. Permeability P_s and diffusion coefficient within a homogeneous cellulose acetate membrane D_{sm} as functions of the external phenol concentration c'_s at 25°C.

TABLE III
Transport Parameters of the Kedem–Spiegler Relationships

Membrane	c_s' (wt-%)	$\Pi' \cdot 10^2$ (atm)	r_∞	$l_p \cdot 10^6$ (cm/s·atm)	$(P_s/d) \cdot 10^4$ (cm/s)
CA-60	0.1	15.5	-0.147	19.11	81.92
CA-75	0.1	15.5	-0.117	13.53	16.65
CA-80	0.1	15.5	-0.283	9.37	23.57
CA-82.5	0.1	15.5	-0.250	5.64	9.10
CA-85	0.1	15.5	-0.211	3.68	4.06
CA-90	0.1	15.5	-0.594	1.15	4.69
F 700	0.05	7.53	-0.851	0.268	0.86
K 700/1	0.05	7.53	-1.159	0.398	1.41
K 700/2	0.05	7.53	-1.200	0.083	0.23
L 700	0.05	7.53	-1.962	0.454	2.64
E 320	0.05	7.53	-4.375	1.068	16.77

diffusion coefficient is calculated by assuming the transport of phenol to take place only in the internal liquid phase of the CA membrane, the result is $D'_{sm} \simeq (9.5 \pm 0.6) \times 10^{-9}$ cm^2/sec utilizing a water content of the homogeneous CA membrane of $w' \simeq 0.15$ g H_2O/cm^3 wet membrane.

Hyperfiltration Data

The computed transport parameters of each of the four theoretical approaches are shown in Tables III–VI, along with the corresponding conditions of the hyperfiltration experiments. The osmotic pressures of the phenol feed solutions shown were taken from the literature.[34] These transport parameters may be used to regenerate the flux and rejection of phenol as functions of the pressure difference across the membrane.

TABLE IV
Transport Parameters of the Combined Viscous Flow–Frictional Relationships

Membrane	$l_p \cdot 10^6$ (cm/s·atm)	K_s'/b	$\delta \cdot f_{sw} \cdot 10^{-7}$ (cm^2·s·atm/mole)	b	$f_{sw} \cdot 10^{-12}$ (cm·s·atm/mole)	$f_{sm} \cdot 10^{-12}$ (cm·s·atm/mole)	b^+[a]
CA-60	19.11	1.15	0.3	34.8	0.29	9.7	17.7
CA-75	13.53	1.12	1.5	35.7	1.23	36.1	18.2
CA-80	9.37	1.28	1.2	31.3	0.57	17.2	15.9
CA-82.5	5.64	1.25	3.1	32.0	0.86	26.5	16.3
CA-85	3.68	1.21	6.7	33.1	1.29	41.4	16.8
CA-90	1.15	1.59	7.6	25.2	0.43	10.7	12.8
F 700	0.268	1.85	48.2	27.6	0.80	21.4	
K 700 (4.5 μm)	0.398	2.16	34.3	18.5	0.76	13.3	
K 700 (25 μm)	0.083	2.20	214.3	18.2	0.86	14.7	
L 700	0.454	2.96	25.1	11.5	0.42	4.39	
E 320	1.068	5.38	7.2	3.5	0.13	0.32	

[a] b^+ was calculated using $K_s' = 16$

TABLE V
Transport Parameters of the Phenomenological Relationships of Thermodynamics of Irreversible Processes

Membrane	c_s' (wt-%)	$\Pi' \cdot 10^2$ (atm)	r_∞	$l_p \cdot 10^6$ (cm/s·atm)	$(l_\pi/l_p) \cdot 10^{-2}$	$l_\pi \cdot 10^3$ (cm/s·atm)
CA-60	0.1	15.5	-0.167	18.32	25.88	47.41
CA-75	0.1	15.5	-0.185	13.34	11.27	15.04
CA-80	0.1	15.5	-0.250	9.06	10.68	9.68
CA-82.5	0.1	15.5	-0.370	5.30	14.65	7.72
CA-85	0.1	15.5	-0.441	3.70	14.50	5.37
CA-90	0.1	15.5	-0.670	1.12	23.20	2.59
F 700	0.05	7.53	-0.952	0.274	37.61	1.03
K 700/1	0.05	7.53	-1.374	0.396	45.59	1.80
K 700/2	0.05	7.53	-1.398	0.077	40.13	0.31
L 700	0.05	7.53	-2.807	0.484	87.63	4.24
E 320	0.05	7.53	-5.531	1.131	215.19	24.55

A comparison of the values of P_s/d, the normalized solute permeabilities, as calculated from different transport relationships, is shown in Table VII. Although there are no P_s/d values listed for the phenomenological relationships in Table V, they can be calculated from:

$$P_s/d = (l_\pi/l_p - r_\infty^2) l_p \Pi' \tag{25}$$

The thickness d of the membrane is required in the calculation of P_s. Although directly measurable for homogeneous CA membranes, d can only be estimated in the case of asymmetric CA membranes. One method of estimation assumes an inverse proportionality between membrane thickness and volume flux, so that the effective thickness of the active layer in an asymmetric membrane can be calculated by comparing its hydrodynamic permeability to that of a homogeneous CA membrane of known thickness:

$$d_{\text{eff}} = \frac{l_p^{\text{hom}}}{l_p^a} d_{\text{hom}} \tag{26}$$

TABLE VI
Transport Parameters of the Extended Solution-Diffusion Model Relationships

Membrane	c_s' (wt-%)	$\Pi' \cdot 10^2$ (atm)	r_∞	$l_p \cdot 10^6$ (cm/s·atm)	$(P_s/d) \cdot 10^4$ (cm/s)	$l_{sp} \cdot 10^{12}$ (mole/cm^2·s·atm)
CA-60	0.1	15.5	-0.167	18.76	73.48	233
CA-75	0.1	15.5	-0.185	13.46	23.30	169
CA-80	0.1	15.5	-0.250	9.22	15.00	122
CA-82.5	0.1	15.5	-0.370	5.69	12.03	82.6
CA-85	0.1	15.5	-0.441	3.65	8.35	55.8
CA-90	0.1	15.5	-0.670	1.16	4.06	20.5
F 700	0.05	7.53	-0.952	0.268	0.78	2.77
K 700/1	0.05	7.53	-1.374	0.398	1.358	5.01
K 700/2	0.05	7.53	-1.398	0.082	0.23	0.97
L 700	0.05	7.53	-2.807	0.455	3.19	9.18
E 320	0.05	7.53	-5.531	1.070	18.45	37.04

The effective thicknesses of the asymmetric CA membranes listed in Table VII were calculated in this way. The possibility of porosity or water content differences between a homogeneous membrane and the active layer of an asymmetric membrane has not been considered in this inverse proportionality. Nevertheless, the values of d_{eff} still appear reasonable compared to independent measurements using electron microscopy,[35] and an approximate value in the range of $0.1\ \mu m < d < 0.5\ \mu m$ may be accepted.

The P_s/d values obtained for a homogeneous CA membrane by using the transport parameter l_π agree well with those of the Kedem–Spiegler and extended solution–diffusion model relationships. All are consistent with the permeability value of phenol obtained from the present dialysis experiments. Moreover, the P_s/d values of the asymmetric CA membranes decrease with increasing annealing temperature, indicating an increase in the thickness of the active layer and a decrease of the water content (porosity) of the active layer with increasing annealing temperature. This observation also agrees with previous experimental and theoretical results.[15] The P_s values of the homogeneous CA membranes calculated using the measured thickness decreases drastically with increasing acetyl content. For example, $P_s \simeq 4.7 \times 10^{-8}$ cm^2/sec for F-700 (40.1 wt % acetyl) and 103×10^{-8} cm^2/sec for E-320 (32.0 wt % acetyl). On the other hand, the P_s values of the asymmetric and homogeneous CA membranes cast from Bayer Cellit K-700 vary vetween 3×10^{-8} and 9×10^{-8} cm^2/sec, indicating that P_s is essentially unaffected by the membrane structure. Since no turtuosity factor was taken into account, however, a small systematic variation of P_s with the density of the membrane or its porosity might still exist.

The nature of the solute diffusion coefficient is the same in all transport relationships. In addition to solute and solvent diffusion, a convective transport of solute and solvent is considered in all transport relationships based on the finely porous membrane model. On the other hand, the extended solution–

TABLE VII
Effective Membrane Thickness d_{eff} and P_s/d Values Calculated from the Various Transport Relationships[a]

Membrane	$d_{eff} \cdot 10^4$ (cm)	$(P_s/d) \cdot 10^4$ (cm/s) KS	$(P_s/d) \cdot 10^4$ (cm/s) TI	$(P_s/d) \cdot 10^4$ (cm/s) Ex-SD	$(P_s/d) \cdot 10^4$ (cm/s) exp
CA-60	0.105	81.92	73.49	73.48	–
CA-75	0.144	16.65	23.33	23.30	–
CA-80	0.212	23.57	15.00	15.00	–
CA-82.5	0.362	9.10	11.96	12.03	–
CA-85	0.519	4.06	8.33	8.35	–
CA-90	1.714	4.69	4.02	4.06	–
F 700	6.0	0.86	0.78	0.78	–
K 700	4.5	1.41	1.36	1.36	1.27
K 700	25.0	0.23	0.23	0.23	0.23
L 700	6.0	2.64	3.19	3.19	–
E 320	5.6	16.77	18.44	18.45	–

[a] KS = Kedem-Spiegler TI = Thermodynamics of Irreversible Processes
Ex-SD = Extended Solution-Diffusion Model

TABLE VIII
Diffusion Coefficients within the Membranes Calculated by Means of the Transport Parameters of the Extended Solution-Diffusion Model

Membrane	c_S^1 (wt-%)	$D_{sp} \cdot 10^{11}$ (cm^2/s)	$D_{sm} \cdot 10^9$ (cm^2/s)	$(D_{sp}/D_{sm}) \cdot 10^3$	$(\bar{V}_w \cdot \tilde{c}_s \cdot K_S^1) \cdot 10^3$	$D_w \cdot 10^6$ (cm^2/s)	$D_w^* \cdot 10^6$ (cm^2/s)	$(D_w^*/w') \cdot 10^6$ (cm^2/s)
CA-60	0.1	0.974	1.52	6.4	10.5	0.268	0.209	1.39
CA-75	0.1	1.14	0.66	17.3	10.6	0.263	0.205	1.37
CA-80	0.1	1.21	0.63	19.4	10.9	0.266	0.207	1.38
CA-82.5	0.1	1.40	0.86	16.4	11.5	0.280	0.218	1.45
CA-85	0.1	1.36	0.85	16.0	11.8	0.257	0.200	1.33
CA-90	0.1	1.65	1.37	12.1	12.7	0.270	0.210	1.40
F 700	0.05	0.780	0.719	10.9	8.9	0.219	0.175	1.31
K 700/1	0.05	1.06	1.20	8.8	7.7	0.243	0.189	1.26
K 700/2	0.05	1.14	1.13	10.1	7.7	0.279	0.217	1.45
L 700	0.05	2.80	4.42	6.3	8.7	0.402	0.309	1.97
E 320	0.05	9.72	43.8	2.2	8.8	0.814	0.529	2.20

diffusion model employs pressure diffusion of the solute and solvent, in addition to normal diffusion, neglecting convective transport entirely. The corresponding pressure diffusion coefficients are not independent transport parameters but are related to the normal diffusion coefficients. In contrast to the extended solution-diffusion model, the finely porous membrane models possess an independent third transport parameter characterizing the convective solute transport by the asymptotic rejection of the membrane. A compilation of the different transport parameters is shown in Table VIII for data analyzed using the extended

TABLE IX
Estimated Partial Molar Volumes $\bar{V}_s$ of Phenol in Various Cellulose Acetate Membranes[a]

Membrane	$\bar{V}_S$ (cm^3/mol)		
	1	2	3
CA-60	72	67	67
CA-75	166	152	152
CA-80	186	121	115
CA-82.5	157	99	93
CA-85	153	95	89
CA-90	46	27	25
F 700	162	90	82
K 700/1	169	86	77
K 700/2	207	106	94
L 700	132	54	45
E 320	92	28	22

[a] $\bar{V}_S$ calculated from Equation (27) by use of:
1. $\tilde{c}_S/c_S^1 = 1$; 2. $\tilde{c}_S/c_S^1 = -r_\infty/\ln(1 - r_\infty)$;
3. $\tilde{c}_S/c_S^1 = (1/2)(2 - r_\infty)$.

solution–diffusion concept. The diffusion coefficients for the solute, D_{sp} and D_{sm}, and those for water, D_w, D_w^*, and D_w^*/w', are listed for all membranes tested. Except in the case of the poorly annelaed CA-60 membrane, the ratios D_{sp}/D_{sm}, calculated from the individual diffusion coefficients, agree reasonably well with that predicted using eq. (17).

DISCUSSION

Model-independent transport relationships may be used to obtain characteristic parameters which allow reconstruction of flux and rejection as functions of the transmembrane pressure drop under hyperfiltration conditions. In this respect, the generality of the phenomenological and Kedem–Spiegler relationships is again well illustrated by the satisfactory fit to the data of the phenol–CA membrane system. As always, however, no insight into the transport mechanism is offered by either approach of data analysis.

Other than the normal solution–diffusion model, the finely porous membrane model is perhaps the simplest among model-dependent relationships discussed. Solute–membrane interactions and pressure diffusion are not considered, and the asymptotic rejection is thus only determined by the solute partition coefficient of the feed solution side, $r_\infty = 1 - K_s$. Substituting actual values of K_s from phenol sorption experiments shows, however, that the simple equation predicts a much more negative rejection than the observed r_∞ values would suggest. This predicted negative rejection would increase further if pressure diffusion were incorporated into the finely porous membrane model. The discrepancy is thus most logically attributed to the strong interaction between phenol and cellulose acetate. This model is therefore unsuited to analyze the present organic solute system.

The viscous flow–frictional model incorporates the drag factor b. The phenol–CA interaction is accounted for by the relative magnitudes of friction coefficients between solute and solvent, f_{sw}, and between solute and membrane, f_{sm}. The values of these parameters for each membrane are shown in Table IV. Equation (10) does not yield a unique pair of K_s, b values for each given r_∞. To solve for b, therefore, K_s must be known or assumed. For homogeneous and asymmetric CA membranes prepared from Bayer Cellit K-700, the respective values of K_s are 40 and 16 (based on the weight of the wet membrane). Two values of b have thus been calculated from these limits for each asymmetric CA membrane, as shown in Table IV. In all cases, b is much larger than 1, or $f_{sm} \gg f_{sw}$, consistent with the notion that much stronger interactions exist between phenol and CA than between phenol and water. As interpreted by the combined viscous flow–frictional model, the negative rejection is a consequence of the favorable partitioning of phenol toward the CA membrane phase.

The alternative approach of the extended solution–diffusion model yields a rather different picture of phenol transport. As with the conventional solution–diffusion model, the extended model assumes no convective contribution to the overall phenol flux. Rather, the negative rejection must be explained in terms of "pressure diffusion" of the solute. A high l_{sp} value results from a high K_s value, so that the pressure diffusion flux is again directly related to the solute partition coefficient.

To justify the validity of the pressure diffusion concept, the partial molar

volume $\overline{V}_s$ of the solute has been calculated by substituting independently determined values of r_∞, P_s/d, and l_p (see Appendix A) into the following equation derived by combining eqs. (15), (16), and (17):

$$\frac{(1 - r_\infty) l_p RT c_s'}{\tilde{c}_s (P_s/d)} = \overline{V}_s \tag{27}$$

where the mean concentration $\tilde{c}_s$ can be obtained from the following relationship:[33]

$$\frac{\tilde{c}_s}{c_s'} = \frac{-r_\infty}{\ln (1 - r_\infty)} \tag{28}$$

An equation similar to eq. (27) has been derived previously by Staverman et al.[37] and Kedem[38] as follows:

$$1 - \sigma = \frac{K_s D_{sm} \overline{V}_s}{D_w' \overline{V}_w w}$$

Using the relation $D_w' \overline{V}_w w = RTl_p$, this equation can easily be transformed into

$$\frac{(1 - \sigma) RTl_p}{P_s/d} = \overline{V}_s$$

Now, introducing the relation $(1 - r_\infty)/(1 - \sigma) = \tilde{c}_s/c_s'$ given previously,[16] eq. (27) results.

Theoretically, there are only two independent variables in the extended solution–diffusion model, namely, P_s/d and l_p. Equation (27) would therefore not yield a realistic $\overline{V}_s$ if an "incompatible" value of r_∞ is additionally specified. The fact that the partial molar volumes so calculated, as listed in Table IX, agree reasonably well with the known value of 94 cm^3/mole for phenol suggests that the values of the parameters used in the substitution were realistic. Some membranes listed do not yield satisfactory $\overline{V}_s$ values regardless of the choice of $\tilde{c}_s/c_s'$ assumptions. These include several of the asymmetric CA membranes and one homogeneous membrane, L-700, possessing a higher water permeability so that convective phenol transport might, in addition to diffusion, be present.

Trial application of eq. (27) to hyperfiltration data involving inorganic salts and asymmetric CA or homogeneous cation exchange membranes results in $\overline{V}_s$ values as high as 100 to 400 cm^3/mole, as opposed to the known partial molar volume of about 18 cm^3/mole for NaCl.[39] This suggests that pressure diffusion is practically nonexistent with inorganic salts as permeants.

The same conclusion can be reached by analyzing eq. (21) which applies only to binary solutions. Since water and salts have about the same partial molar volumes, eq. (21) indicates that the ratio D_p/D_s will be rather small. By contrast, $\overline{V}_s - \overline{V}_w$ for a phenol–water system can be as high as 300 times larger than for a salt–water system, leading to a much more significant pressure diffusion coefficient for phenol. These considerations tend to support the validity of the extended solution–diffusion model as an alternative theoretical approach.

The estimated phenol diffusion coefficients increase with increasing water content in the different homogeneous CA membranes or with decreasing annealing temperature for the asymmetric CA membranes. Depending upon the water content of the membranes, diffusion coefficients of phenol range from 9.0

$\times 10^{-10}$ up to about 1.0×10^{-6} cm^2/sec based on the geometric area of the membrane. The diffusion coefficients obtained for the asymmetric membranes are of the same order of magnitude as those of the corresponding homogeneous CA membrane, K-700. All the estimated diffusion coefficients of phenol and their dependence on the water content of the membranes match well with the concept of diffusion through narrow pores. Furthermore, the phenol diffusion coefficients estimated for the asymmetric CA membranes are of the same order of magnitude as those obtained for salts from the corresponding hyperfiltration data.[14,15]

Finally, it is interesting to examine the diffusion coefficients of water within the different membranes, as shown in Table VIII. The water diffusion coefficients D_w, D_w^*, and D_w^*/w' increase with increasing water content of the homogeneous CA membranes. However, the normalized diffusion coefficient D_w^*/w', based on the fixed center of mass frame of reference, varies much less than the two other diffusivities and ranges from about 1.3×10^{-6} to about 2.2×10^{-6} cm^2/sec. The values of the normalized diffusion coefficient are about $1/10$ of the self-diffusion coefficient of water in bulk water, which is about $D_w^s \simeq 2.5 \times 10^{-5}$ cm^2/sec, indicating that either a large turtuosity factor has to be considered or that the membrane matrix with its narrow pores leads to a strong hindrance of the water movement.

Using the determined transport coefficients and the corresponding transport relationships, the solute rejection r can be calculated as a function of the pressure difference across the membrane. Some typical results of such calculations are graphically represented in Figures 6(a)–6(c). As can be seen, the agreement between calculated and measured values of r is satisfactory. The mean errors of the calculated values of r are given in Table X for the transport relationships and membranes used. The large errors are mainly due to the limited accuracy in concentration determination. The differential refractometer used allows for an accuracy of about 0.5–1% of the value of c_s. Because of the similarity in feed and product concentrations, the accuracy of concentration measurement results therefore in an accuracy in r no better than ±10–40%. Phenol rejection at lower pressure differences across the membrane will thus be subject to much larger errors.

CONCLUSIONS

The transport of organic solutes such as phenol can be described by two membrane model relationships, namely, the combined viscous flow–frictional model and the extended solution–diffusion model introduced in this paper. In addition, the membrane model-independent transport relationships, the Kedem–Spiegler relationship and the phenomenological relationship, are as applicable to characterizing the transport of phenol as that of salt across synthetic membranes. The concept of pressure diffusion of the organic solute inherent in the extended solution diffusion model is consistent with the partial molar volumes estimated from the original transport coefficients of the extended solution–diffusion model. The extended solution–diffusion model fails to describe solute transport across synthetic membranes if the water content of the membrane exceeds some limiting value and thus convective flow of the solvent becomes significant. This limitation of the extended solution–diffusion model

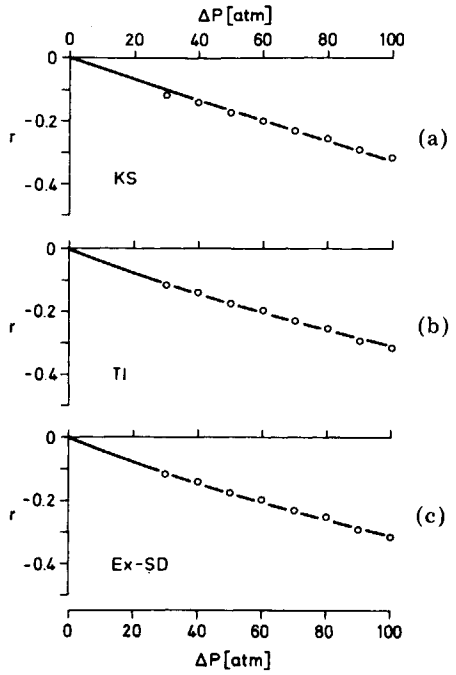

Fig. 6. Phenol rejection r as function of the pressure difference ΔP for a homogeneous cellulose acetate membrane (K 700/1) at 25°C calculated by use of the Kedem–Spiegler relationship (a), the phenomenological relationship (b), and the extended solution–diffusion model relationship (c) as well as the corresponding transport parameters. The points are the measured values of r.

is also well known for the common solution–diffusion model developed by Merten et al. and has the same physicochemical origin in both cases, viz., the presence

TABLE X
Mean Error Δ of the Calculated Phenol Rejection r for the Different Transport Relationships and Membranes Used[a]

Membrane	Δ_{KS}	Δ_{TI}	Δ_{Ex-SD}
CA-60	33.4 %	36.3 %	38.2 %
CA-75	9.3 %	9.1 %	7.5 %
CA-80	9.1 %	16.8 %	18.0 %
CA-82.5	12.9 %	13.1 %	12.0 %
CA-85	11.1 %	11.3 %	10.7 %
CA-90	11.3 %	15.1 %	13.6 %
F 700	5.9 %	5.9 %	5.3 %
K 700 (4.5 μm)	6.5 %	3.0 %	3.1 %
K 700 (25 μm)	7.3 %	7.5 %	7.3 %
L 700	2.1 %	2.0 %	1.6 %
E 320	2.2 %	2.1 %	2.3 %

[a] KS = Kedem-Spiegler
TI = Thermodynamics of Irreversible Processes
Ex-SD = Extended Solution-Diffusion Model

of larger pores in the membrane leading to convective permeation rates which are much larger than the diffusion rates.

The experimental and theoretical results of this work support the assumption underlying the finely porous membrane model. The finely porous membrane model and its modifications yield an adequate description of solute and solvent transport across synthetic membranes. It should be noted that pressure diffusion could also be incorporated into the finely porous membrane model. In the limiting case of very narrow pores, the concept of pores becomes a matter of semantics.[40,41] In this limiting case, the finely porous membrane model merges into the solution–diffusion model. Therefore, the solution–diffusion model and its extended version are able to characterize solute and solvent transport across synthetic membranes consistently. In general, in the presence of strong solute–membrane interactions, the combined viscous flow and frictional model can be used in characterizing the transport behavior. However, if large differences in the partial molar volumes of solute and solvent exist, the extended solution–diffusion model is also an adequate description of the transport phenomena.

The authors are grateful to Professor R. Schlögl for his interest in this work. Furthermore, Mrs. B. Bäppler, Mr. H. Hildebrandt, and Mrs. H. Müller are thanked for their assistance in carrying out the hyperfiltration and sorption measurements. Mr. R. Gröpl is acknowledged for his expert preparation of the membranes used in this study. The work was supported financially by the Bundesminister für Forschung und Technologie, Bonn, Germany.

APPENDIX A

In order to determine the transport parameters P_s/d and l_p of the extended solution–diffusion model, the following procedure should in principle be performed. The value of P_s/d is obtained from the slope of the $1/r$ vs. $1/q$ regression line. In addition, the intersection of this regression line with the ordinate yields a first approximation of r_∞. The hydrodynamic permeability l_p is obtained from the slope of the q vs. $(\Delta P - \Delta\Pi)$ regression line. The values of P_s/d and l_p thus determined are then inserted into eq. (27), yielding a second value of r_∞ on the premises that $\overline{V}_s$, the partial molar volume of the solute in the membrane, is known. With this value of r_∞ the regression line analysis of the following relationship is performed again in order to determine a second value of P_s/d:

$$\frac{r_\infty - r}{r} = \frac{P_s}{d}\frac{1}{q} \tag{14a}$$

This process has then to be iterated till the values of r_∞, l_p, and P_s/d, being not independent from each other, are consistent with eq. (27).

This iterative procedure might be somewhat cumbersome. Therefore, the following more convenient determination of the transport parameters might be adopted. This procedure must be performed especially when the value of $\overline{V}_s$ in the membrane is expected to deviate strongly from that in the bulk solution and is not known from independent measurements. Assuming r_∞ to be a third independent transport parameter, the aforementioned regression lines are calculated using the experimental data of q and r as functions of ΔP. The values of r_∞, l_p, and P_s/d obtained by this regression line analysis are then again inserted into eq. (27), and the corresponding value of $\overline{V}_s$ is obtained. If this calculated value of $\overline{V}_s$ agrees reasonably well with the known or expected value of the partial molar volume of the solute in the membrane, the set of the three transport parameters r_∞, l_p, and P_s/d is considered to be consistent with the solution–diffusion model relationships. This procedure was adopted in this paper. In case that the value of $\overline{V}_s$ calculated along these lines deviates strongly from the real value or the one expected for the partial molar volume of the solute in the membrane, the extended solution–diffusion model relationships might be considered unfit with the experimental data. More appropriate model relationships have then to be applied beside the model independent transport relationships.

APPENDIX B

In order to quantify the sorption of phenol by an analytical relationship and thus gain a deeper insight into phenol sorption by CA membranes on a molecular level, a sorption model might be used. Assuming phenol sorption by CA membranes to take place by means of strong interactions between phenol molecules and sorption sites of the CA chains and considering, in addition, the sorbed phase as a two-dimensional gas, phenol sorption can be related to a gain in surface energy at the polymer–solution interface.[29] Originally developed for the sorption of vapors by polymers, this sorption model is applied on approval to the sorption of a solute if the solute partition is highly in favor of the polymer phase, as is the case for the phenol–CA membrane system within the range of phenol concentrations used. Applying an equation for multilayer adsorption (eq. 30 of ref. 29), a least-squares analysis of corresponding experimental sorption data yields $n = 1$ for the number of sorbed layers. Employing that value of $n = 1$, the multilayer sorption isotherm is reduced to a monolayer sorption isotherm identical to a Freundlich-type isotherm[29]:

$$u = u_m c_s^{1/a} \tag{B-1}$$

where u_m is the amount of phenol sorbed at an external phenol concentration of $c_s = 1$ mole/l., thus yielding a measure of the monolayer capacity. The model parameter a is related to the gain in molar surface energy of the system, e, as follows:

$$a = \frac{e}{RT} \tag{B-2}$$

where R is the gas constant (l. atm/mole degree) and T is the temperature in K. The model parameters u_m and a can easily be obtained from the intercept and slope of a plot of log u vs. log c_s. It should be pointed out that while the sorbent is assumed to behave as a two-dimensional gas, the existence of a geometric surface within the polymer phase is not required. Rather, the sorbed molecules may still be distributed throughout the bulk phase of the polymer, but their statistical distribution is restricted to two dimensions along the polymer chains. This implies that the mobility of the phenol molecules beyond the two dimensions is statistically negligible because of geometric and energetic restrictions. This concept of sorbed molecules mobile in two dimensions differs clearly from the Langmuir and BET model with localized layers of sorbed molecules.

References

1. R. Blunk, A Study of Criteria for the Semipermeability of Cellulose Acetate Membranes to Aqueous Solutions, UCLA Water Resources Center Rept., WRCC 88, 1964; also UCLA Dept. of Engineering Rept. 64-28, 1964.
2. B. Keilin, OSW, Res. & Develop. Propr. Rept. No. 117, Aerojet-General Corp., 1964.
3. H. K. Lonsdale, U. Merten, and M. Tagami, *J. Appl. Polym. Sci.*, **11**, 1807 (1967).
4. T. Matsuura and S. Sourirajan, *J. Appl. Polym. Sci.*, **15**, 2905 (1971).
5. T. Matsuura and S. Sourirajan, *J. Appl. Polym. Sci.*, **16**, 2531 (1972).
6. J. E. Anderson, S. J. Hoffman, and C. R. Peters, *J. Phys. Chem.*, **76**, 4006 (1972).
7. G. Jonsson, *Desalination*, **24**, 19 (1978).
8. W. Pusch, H.-G. Burghoff, and E. Staude, *Proceedings of the 5th International Symposium on Fresh Water from the Sea*, Vol. 4, A. Delyannis and E. Delyannis, Eds., Athens, 1976, p. 143.
9. G. Schmid, *Z. Elktrochem.*, **54**, 424 (1950).
10. R. Schlögl, *Z. Phys. Chem., N.F.*, **1**, 305 (1954); *Ber. Bunsenges. Phys. Chem.*, **70**, 400 (1966).
11. G. Jonsson and C. E. Boesen, *Desalination*, **17**, 145 (1976).
12. W. Pusch and R. Riley, *Desalination*, **22**, 191 (1977).
13. E. Oikawa and T. Ohsaki, *Desalination*, **25**, 187 (1978).
14. W. Pusch, *Ber. Bunsenges. Phys. Chem.*, **81**, 854 (1977).
15. W. Pusch, *Proceedings of the 6th International Symposium on Fresh Water from the Sea*, Vol. 3, A. Delyannis and E. Delyannis, Eds., Athens, 1978, p. 247.
16. W. Pusch, *Ber. Bunsenges. Phys. Chem.*, **81**, 854 (1977).
17. O. Kedem and K. S. Spiegler, *Desalination*, **1**, 311 (1966).
18. U. Merten, in *Desalination by Reverse Osmosis*, U. Merten, Ed., M.I.T. Press, Cambridge, MA, 1966, p. 25; H. K. Lonsdale, U. Merten, R. Riley, K. D. Vos, and J. C. Westmoreland, Reverse Osmosis for Water Desalination, OSW, Res. & Develop. Progr. Rept. No. 16, PB 161391, 1957.

19. E. H. Bresler, E. A. Mason, and R. P. Wendt, *Biophys. Chem.*, **4,** 229 (1976); E. H. Bresler and R. P. Wendt, *Science,* **163,** 944 (1969); **166** 1437 (1969).

20. K. S. Spiegler, *Trans. Faraday Soc.*, **54,** 1408 (1958).

21. W. E. Clark, *Science,* **138,** 148 (1963).

22. R. Haase, *Thermodynamik der irreversiblen Prozesse,* Dr.-Dietrich-Steinkopff-Verlag, Darmstadt, 1963, pp. 354–55.

23. I. Prigogine, *Etude Thermodynamique des Phénomènes irréversibles,* Desoer, Paris-Liège, 1947, p. 89.

24. P. Bo and V. Stannett, *Desalination,* **18,** 113 (1976).

25. R. Schlögl, *Stofftransport durch Membranen,* Dr.-Dietrich-Steinkopff-Verlag, Darmstadt, 1966, pp. 100–101.

26. S. Manjikian, S. Loeb, and J. W. McCutchan, Proceedings of the 1st Int. Desalination Symposium, Paper SWD/12, Washington, D.C., 1965.

27. W. Pusch, *Desalination,* **16,** 65 (1975).

28. B. Baum, St. A. Margosiak, and W. H. Holley, Study of Methods to Retard Compaction of Cellulose Acetate Membranes in Reverse Osmosis Desalination, OSW, Res. & Develop. Progr. Rept. No. 467, October 1969.

29. H.-G. Burghoff and W. Pusch, *J. Appl. Polym. Sci.*, **24,** 1479 (1979).

30. H.-G. Burghoff and W. Pusch, *J. Appl. Polym. Sci.*, **23,** 473 (1979).

31. H.-G. Burghoff and W. Pusch, *J. Appl. Polym. Sci.*, **20,** 789 (1976).

32. H. K. Lonsdale, U. Merten, and R. L. Riley, *J. Appl. Polym. Sci.*, **9,** 1341 (1965).

33. A. Katchalsky and P. F. Curran, *Nonequilibrium Thermodynamics in Biophysics,* Harvard University Press, Cambridge, MA, 1965, p. 118.

34. A. Grollman and J. C. W. Frazer, *J. Am. Chem. Soc.*, **45** 1705 (1923).

35. R. L. Riley, U. Merten, and J. O. Gardner, *Desalination,* **1,** 30 (1966).

36. H. K. Lonsdale, U. Merten, R. L. Riley, K. D. Vos, and J. C. Westmoreland, Reverse Osmosis for Water Desalination, OSW, Res. & Develop. Progr. Rept. No. 111, May 1964.

37. J. L. Thalen and A. J. Staverman, *Trans. Faraday Soc.*, **61,** 2794 (1965).

38. O. Kedem and A. Katchalsky, *Biochem. Biophys. Acta,* **27,** 229 (1958).

39. B. M. Fabuss, Thermodynamic Properties of Saline Water, OSW, Res. & Develop. Progr. Rept. No. 136, July 1965.

40. W. Kuhn, *Z. Elektrochem.*, **55,** 207 (1951).

41. S. A. Stern, private communication.

Received August 15, 1979